Cell Death & Differentiation (2020) 27:1475–1488
https://doi.org/10.1038/s41418-019-0430-6

Cell Death & Differentiation

ARTICLE

miR17~92 restrains pro-apoptotic BIM to ensure survival of haematopoietic stem and progenitor cells

Kerstin Brinkmann[1,2] · Ashley P. Ng[1,2] · Carolyn A. de Graaf[1,2] · Ladina Di Rago[1] · Craig D. Hyland[1] · Eugenio Morelli[3,4] · Jai Rautela[1,2,5] · Nicholas D. Huntington[1,2,5] · Andreas Strasser[1,2] · Warren S. Alexander[1,2] · Marco J. Herold[1,2]

Received: 5 July 2019 / Revised: 22 September 2019 / Accepted: 23 September 2019 / Published online: 7 October 2019

Abstract

The *miR17~92* cluster plays important roles in haematopoiesis. However, it is not clear at what stage of differentiation and through which targets *miR17~92* exerts this function. Therefore, we generated *miR17~92*$^{fl/fl}$*; RosaCreERT2* mice for inducible deletion of *miR17~92* in haematopoietic cells. Bone marrow reconstitution experiments revealed that *miR17~92*-deleted cells were not capable to contribute to mature haematopoietic lineages, which was due to defects in haematopoietic stem/progenitor cells (HSPCs). To identify the critical factor targeted by *miR17~92* we performed gene expression analysis in HSPCs, demonstrating that mRNA levels of pro-apoptotic *Bim* inversely correlated with the expression of the *miR17~92* cluster. Strikingly, loss of pro-apoptotic BIM completely prevented the loss of HSPCs caused by deletion of *miR17~92*. The *BIM/miR17~92* interaction is conserved in human CD34^{+} HSPCs, as *miR17~92* inhibition or blockade of its binding to the *BIM* 3′UTR reduced the survival and growth of these cells. Despite the prediction that *miR17~92* functions by impacting a plethora of different targets, the absence of BIM alone is sufficient to prevent all defects caused by deletion of *miR17~92* in haematopoietic cells.

Introduction

MicroRNAs (miRNAs) regulate many biological processes by binding and post-transcriptionally regulating multiple different gene products [1, 2]. However, currently the regulation of gene products by a specific miRNA is mostly based on prediction and overexpression assays but often lacks the study of physiological functions within a whole organism.

The *miR17~92* cluster consists of *miR17*, *miR18a*, *miR19a*, *miR20a*, *miR19b1* and *miR92-1*, which belong to four different seed families [3]. Studies of mice constitutively deficient for *miR17~92* revealed that this microRNA cluster is essential for the normal development of several organs, including the heart, lung and skeleton, as well as for the production of B and T lymphocytes [4–8]. Mice deficient for *miR17~92* (*miR17~92*$^{del/del}$) die soon after birth owing to severe lung and ventricular septal defects [5]. Conditional deletion using tissue-specific CRE transgenes revealed that the *miR17~92* cluster also plays a critical role in the development of several haematopoietic cell populations [9–12]. Accordingly, haematopoietic stem/progenitor cells (HSPCs) from the foetal livers of *miR17~92*$^{del/del}$ embryos (E14.5) produced substantially fewer pro-B/pre-B cells compared with wild-type HSPCs when transplanted into lethally irradiated recipient mice [5, 13]. Moreover, haematopoietic cell-specific loss of *miR17~92* in *miR17~92*$^{fl/fl}$*; vav-Cre* mice impaired T cell

Supplementary information The online version of this article (https://doi.org/10.1038/s41418-019-0430-6) contains supplementary material, which is available to authorized users.

✉ Marco J. Herold
herold@wehi.edu.au

1 The Walter and Eliza Hall Institute of Medical Research, Melbourne, VIC, Australia

2 Department of Medical Biology, University of Melbourne, Melbourne, VIC, Australia

3 Jerome Lipper Multiple Myeloma Centre, Department of Medical Oncology, Dana Farber Cancer Institute, Boston, MA, USA

4 Harvard Medical School, Boston, MA, USA

5 Present address: Biomedicine Discovery Institute, Department of Biochemistry and Molecular Biology, Monash University, Clayton, VIC, Australia

development both at the level of T cell progenitors in the thymus and at later stages of differentiation [14].

Of note, aberrant expression of the *miR17~92* cluster can contribute to lymphoma development. Overexpression of *miR-17-92* resulted in a lymphoproliferative disorder [6] similar to that observed in mice with loss of pro-apoptotic BIM [15] or overexpression of anti-apoptotic BCL-2 [16, 17]. Moreover, *miR17~92* is overexpressed in certain B cell lymphomas and enforced expression of *miR17~92* accelerated MYC-driven lymphomagenesis in mice [18–21]. In vitro studies indicated that MYC increases the transcription of the *miR17~92* cluster [22], and this is thought to promote tumorigenesis through repression of several genes that promote apoptosis (*Bim*), proliferation and differentiation *(Pten)* [5]. However, the precise functional connections between *miR17~92* and its targets and their relevance for lymphoma development remain unresolved.

Importantly, the studies published thus far do not discriminate whether the loss of the different haematopoietic cell types caused by the deletion of *miR17~92* is due to a direct impact of the loss of this microRNA cluster in these cells or a consequence of its loss in a more primitive stem/progenitor population. To address this question, we generated mice in which *miR17~92* could be inducibly deleted only in haematopoietic cells by using the *RosaCreERT2* transgene and haematopoietic reconstitution studies. Deletion of the *miR17~92* cluster substantially reduced the competitiveness of HSPCs in mixed bone marrow reconstitution experiments. Interestingly, the absence of the pro-apoptotic BH3-only protein BIM, one of many predicted targets of *miR17~92*, completely prevented the defects in the survival of HSPCs that is caused by the deletion of *miR17~92*. These findings demonstrate that *miR17~92* safeguards the survival of HSPCs by restraining the levels of the pro-apoptotic BH3-only protein BIM.

Material and methods

Mice

Experiments with mice (8–12 weeks, male and female) were approved by and conducted according to the guidelines of The Walter and Eliza Hall Institute Animal Ethics Committee. Expert animal technicians were fully blinded to the genotypes and treatments of mice in the experiments. No animals were excluded from any experiment unless technical issues were present. The generation of *miR17~92*$^{fl/fl}$, *Rosa-CreERT2*$^{+/Ki}$, *Bim*$^{-/-}$ and *Puma*$^{-/-}$ mice, all maintained on a C57BL/6-Ly5.2 background, have been described previously [5, 15, 23, 24]. To activate CreERT2, mice were given 60 mg/kg tamoxifen (Sigma-Aldrich, Rowville, VIC, Australia) in peanut oil/10% ethanol each day for 3 days by oral gavage 8–15 weeks post transplantation with bone marrow or foetal liver cells [25].

Haematopoietic reconstitution experiments

Bone marrow or foetal liver cells of the test and competitor populations (GFP) were mixed 1:1 in PBS/10% FCS. A total of 6×10^6 bone marrow cells or $2–5 \times 10^5$ foetal liver cells were injected i.v. into each lethally irradiated (2×5.5 Gy, 3 h between doses) female C57BL/6-Ly5.1 recipient (8–10 weeks, randomly chosen) 2 h after the second dose of γ-irradiation. Retro-orbital bleeds were taken 8 weeks after transplantation to confirm successful haematopoietic reconstitution by determining the frequency of Ly5.2-positive cells by FACS analysis.

Blood and flow cytometric analysis

Haemogram analysis was performed using the ADVIA system. FACS analysis was performed as previously described [26]. HSPCs were analysed by staining with fluorochrome-conjugated monoclonal antibodies against the following cell surface markers: CD150-BV421 (clone TC15-12F12.2, Biolegend), CD127-APC (IL-7 receptor, clone A7R34, eBioscience), CD48-PECy7 (clone HM48-1, eBioscience), CD105-PE (clone MJ718, eBioscience), CD34-A647 (clone RAM34, BD), CD117-BV711 (clone 2B8, BD), CD16/32-PerCPCy5.5 (clone 2.4G2, BD), CD135-PE (eBioscience), CD41-PECy7 (clone MWReg30, BD), SCA-1-A595, CD127-APCCy7 (eBioscience), CD9-A647, CD16_32-FITC, CD41-PECy7, CD2-A700, CD4-A700, CD8-A700, GR-1-A700, F4/80-A700, CD19-A700, B220-A700, Ly6G-A700, TER-119-A700 and NK1.1-A700 [27].

Cell culture

Total bone marrow cells were isolated from the tibia and femur of mice with the indicated genotypes. Bone marrow cells were cultured on OP9 stromal cells in Iscove's Modified Dulbecco's medium (IMDM) containing 10% newborn calf serum (Sigma), 1% BSA, 2 mM glutamine, 50 mM beta-mercaptoethanol and supplemented with 20 ng/mL IL-6. To obtain T-cell blasts, 2×10^6 spleen cells were stimulated with recombinant mIL-2 and 2 µg/mL concanavalin A (ConA) (Sigma) in Dulbecco's modified Eagle's medium supplemented with 10% FCS, 50 mM beta-mercaptoethanol and 100 mM asparagin for 3 days. Subsequently, cells were washed five times to remove ConA and then cultured in the presence of recombinant mIL-2. Cells were cultured in a fully humidified atmosphere of 5% CO_2 in air in the presence or absence of 10 µM 4-Hydroxy-

tamoxifen (Sigma) and 25 nM QVD-OPh (JOMAR LIFE RESEARCH).

RNA extraction and quantitative RT-PCR

RNA was extracted using the standard phenol–chloroform extraction protocol using TRIzol™ (Ambion Inc). Isolated RNA was reverse transcribed using oligo-dT primers and the TaqMan™ Reverse Transcription Kit (Applied Biosystems) and cDNA synthesis was carried out according to the manufacturer's instructions. Quantitative RT-PCR reactions were performed in triplicate using the TaqMan™ gene expression assays (Applied Biosystems) for *Bcl2l11* mRNA (Cat#Mm00437796_m1). Data were collected using the Viia7 PCR System (Thermo Fischer Scientific) using the Viia7™ software package (Thermo Fischer Scientific). Probing for HMBS (Cat#Mm01143545_m1) served as a house-keeping gene. Data were calculated using the $2^{-\Delta\Delta CT}$ method.

Cell lysis and western blotting

Cell lysates were generated using CHAPS lysis buffer (10 mM HEPES, pH 7.4; 150 mM NaCl; 1% CHAPS; complete protease inhibitor cocktail). Protein concentration was determined by Bradford assay using the Protein Assay Dye Reagent Concentrate (Bio-Rad). Proteins were size fractionated by gel electrophoresis on NuPAGE 4–12% Bis-Tris 1.5 mm gels (Life Technologies) in MES buffer and then transferred onto nitrocellulose membranes (Life Technologies) using the iBlot membrane transfer system. The following primary antibodies were diluted in 3% BSA in PBS/0.1%Tween buffer: rabbit anti pAKT (Cell Signalling), AKT (Cell Signalling), BIM (ENZO) and ACTIN (Sigma). Secondary anti-rat/mouse/rabbit IgG antibodies conjugated to HRP (Southern BioTech) were applied, followed by Luminata Forte Western HRP substrate (Millipore) for band visualisation. Membranes were imaged using the ChemiDoc XRS+ machine with ImageLab software (Bio-Rad).

Microarray analyses

Gene expression data from mature haematopoietic cells were taken from the ImmGen dataset (www.immgen.org) [28]. Statistical significance was tested by calculation of Pearson correlation.

Gene deletion analysis using genotyping PCR

Genomic DNA was isolated using tail lysis buffer (Invitrogen). The genotyping PCR reaction detecting miR^{fl} (floxed allele) and miR^{del} (deleted allele) was performed using forward primer (5′ TCGAGTATCTGACAATGTGG) and specific reverse primers detecting the floxed (fl) (5′ TAGCCAGAAGTTCCAAATTGG) or deleted (del) (5′ ATAGCCTGAAACCAACTGTGC) allele. Deletion efficiency was calculated by densitometric analysis of deleted vs. non-deleted PCR products using the Image Lab software (BioRad).

Human HSPC isolation and colony formation assays

Human cord blood-derived $CD34^+$ cells (human HSPCs) were obtained from the Bone Marrow Donor Institute/Cord Blood Research Unit (Murdoch Children's Research Institute, Parkville, VIC, Australia) under approval from The Walter and Eliza Hall Institute of Medical Research Human Research Ethics Committee. $CD34^+$ cells were isolated using immunomagnetic positive selection (Stemcell Technologies #17896) according to the manufacturer's instructions and expanded in complete StemMACS HSC Expansion medium (Miltentyi Biotech 130-100-473 & 130-100-843). 5000 cells were cultured in 1 mL volumes of 0.3% agar in IMDM containing 20% newborn calf serum, 1% BSA, 2 mM glutamine, 0.1 mM 2-mercaptoethanol and supplemented with 50 ng/mL stem cell factor, 20 ng/mL GM-CSF, 20 ng/mL G-CSF, 20 ng/mL IL-3, 20 ng/mL IL-6 and 3 U/mL erythropoietin treated with 20 μM of MIR17PTi [29], scrambled control or no treatment in a fully humidified atmosphere of 5% CO_2 in air. Colonies were fixed, dried onto glass slides, and stained for acetylcholinesterase as well as with Luxol fast blue and haematoxylin, and the numbers of colonies were determined by microscopic examination. The mean of two technical replicates was determined for each treatment, and the proportion of colonies from cells treated with MiR17PTi and scrambled control are shown relative to no drug treatment with mean and standard error of the mean from the analysis of two independent human cord blood samples.

Target protector transfection

Target protectors specific for the four predicted seed regions in the human *BIM 3′UTR* for mature miRNAs of the *miR17~92* cluster were designed using the online tool from Qiagen. Sequences: *miR17* seed: CCAGTCTCCTGAC TAGAGCACTTTACTCTGTTTCCTCAGC, *miR19* seed: CCCTGGCTTACTTGTGTTTTGCACTGATGAATTTTG ACAG, *miR92.1* seed: CTGAGCCAAATGTCTGTGTGC AATTGTGTTTCCTTTACCT, *miR92.2* seed: TAATTGC CACTTTACTTGTGCAATACTGCTGTAAATAACT.

Cells were transfected with 2 μM target protector or scrambled oligos using the Lonza nucleofection kit (P3 primary cell media with supplement 1, DK-100). Cells were co-transfected with pEX-GFP to allow identification of

transfected cells by flow cytometric analysis. At 48 h after transfection, the viability of the transfected cells was assessed by flow cytometric analysis with viable transfected cells defined as $GFP^{+}AnnexinV^{-}DAPI^{-}$.

Results

Deletion of *miR17~92* causes a competitive disadvantage in diverse haematopoietic cell types in vivo that can be rescued by deletion of BIM

To assess the impact of *miR17~92* deletion in adult animals, we generated *miR17~92*$^{fl/fl}$*; RosaCreERT2*$^{+/Ki}$ mice. Upon induction of *miR17~92* deletion by treatment with tamoxifen, we observed no obvious differences in appearance and behavior between these mice and wild-type controls (data not shown). However, we found a significant reduction of various haematopoietic cell populations in the spleen, blood and bone marrow (BM) in *miR17~92*-deleted mice (Supplementary Fig. S1A–C), which is in line with previous reports [5, 6, 13, 14, 30]. The reduction in the various haematopoietic cell types we observed is probably an underestimation of the effects exerted by the loss of *miR17~92*, given that although *miR17~92* deletion in spleen and BM cells was initially almost complete, this was found to be <50% after 1 month (Fig. 1a).

These findings demonstrate an important role of *miR17~92* in haematopoietic cells, but how this microRNA cluster exerts its function in the haematopoietic compartment is not understood. In order to identify the most critical factor targeted by *miR17~92* we performed gene expression analysis using data provided in the ImmGen microarray database (https://www.immgen.org) [28]. This revealed a negative correlation of the expression of *Bim (BCL2L11)* mRNA and the *miR17~92* cluster host gene *(miR17hg)* in all immature and mature lymphoid cell subsets, several haematopoietic progenitor populations and mature cell types of myeloid origin, including macrophages, monocytes and granulocytes (Fig. 1b, Pearson correlation: −0.23, *p*-value < 0.001). Remarkably, this correlation was associated with high expression of *miR17hg* in progenitors, which decreases in lineage-committed cells, with the opposite pattern observed for *Bim mRNA*. A similar pattern was observed upon analysis of murine RNA-Seq data sets that are available in the Haemopedia database (data not shown) [31, 32]. In contrast, no significant correlation was observed in gene expression analysis of *miR17~92* and *Pten*, another recognized target of the *miR17~92* cluster [5, 6, 21], in hematopoietic progenitor populations.

In line with these observations, we noticed a marked upregulation of *Bim* mRNA and BIM protein levels when we deleted *miR17~92* in bone marrow cells in vitro (Fig. 1c and Supplementary Fig. S1D). A similar increase of BIM protein levels (BIM_{EL} and BIM_{L}) were detected upon deletion of *miR17~92* in cultured T cell blasts (Supplementary Fig. S1E). Of note, we did not observe changes in PI3K/AKT signaling upon deletion of *miR17~92*, consistent with the notion that the increase of BIM protein is a direct consequence of the loss of *Bim* regulation by *miR17~92* and not due to an increase in PTEN with a consequent inhibition of PI3K/AKT signaling (Supplementary Fig. S1D).

This prompted us to test whether the deletion of BIM could rescue *miR17~92*-deleted haematopoietic cells by generating *miR17~92*$^{fl/fl}$*; RosaCreERT2*$^{+/Ki}$*; Bim*$^{-/-}$ *mice*. Firstly, we analysed the deletion efficiency of the *miR17~92* cluster in the haematopoietic organs of these mice and control animals after treatment with tamoxifen. While the efficiency of *miR17~92* deletion in haematopoietic cells was significantly <70% at 3 months post tamoxifen-treatment in the *miR17~92*$^{fl/fl}$*; RosaCreERT2*$^{+/Ki}$ mice, almost complete deletion was observed in cells from the bone marrow, spleen, blood and thymus of the *miR17~92*$^{fl/fl}$*; RosaCreERT2*$^{+/Ki}$*;Bim*$^{-/-}$ mice (Fig. 1d). These findings indicate that loss of BIM may be sufficient to rescue the defects in haematopoietic cells that are caused by the deletion of the *miR17~92* cluster.

Loss of pro-apoptotic BIM prevents the reduction in lymphoid, myeloid and erythroid cells that is caused by the induced deletion of *miR17~92*

The findings described above suggest that BIM may be critical for the loss of the haematopoietic cell populations that occurs upon the induced deletion of the *miR17~92* cluster. To examine the functional interaction of *miR17~92* and BIM-mediated apoptosis, we performed competitive bone marrow reconstitution experiments. Lethally irradiated wild-type (wt; C57BL/6-Ly5.1) mice were reconstituted with a 1:1 mixture of GFP-expressing wt (GFP-C57BL/6-Ly5.2) competitor bone marrow cells and test bone marrow cells of the genotypes of interest, i.e. *miR17~92*$^{fl/fl}$*; RosaCreERT2*$^{+/Ki}$ or *miR17~92*$^{fl/fl}$*; RosaCreERT2*$^{+/Ki}$*; Bim*$^{-/-}$ (all on a C57BL/6-Ly5.2 background). After confirming efficient haematopoietic reconstitution of the competitor and the test cells by FACS analysis ~8–10 weeks post-transplantation, the recipient mice were treated with tamoxifen to delete the *miR17~92* cluster in the test cells. These animals were analysed after another 60 days (experimental design depicted in Supplementary Fig. S2A). As predicted, we observed significant reductions in several haematopoietic cell populations, including immature as well as mature B and T cells, myeloid cells and erythroid cells, that had lost the *miR17~92* cluster, whereas wt as well as *RosaCreERT2*$^{+/Ki}$ cells were not outcompeted by the GFP-expressing wt cells (Fig. 2). Remarkably, deletion of

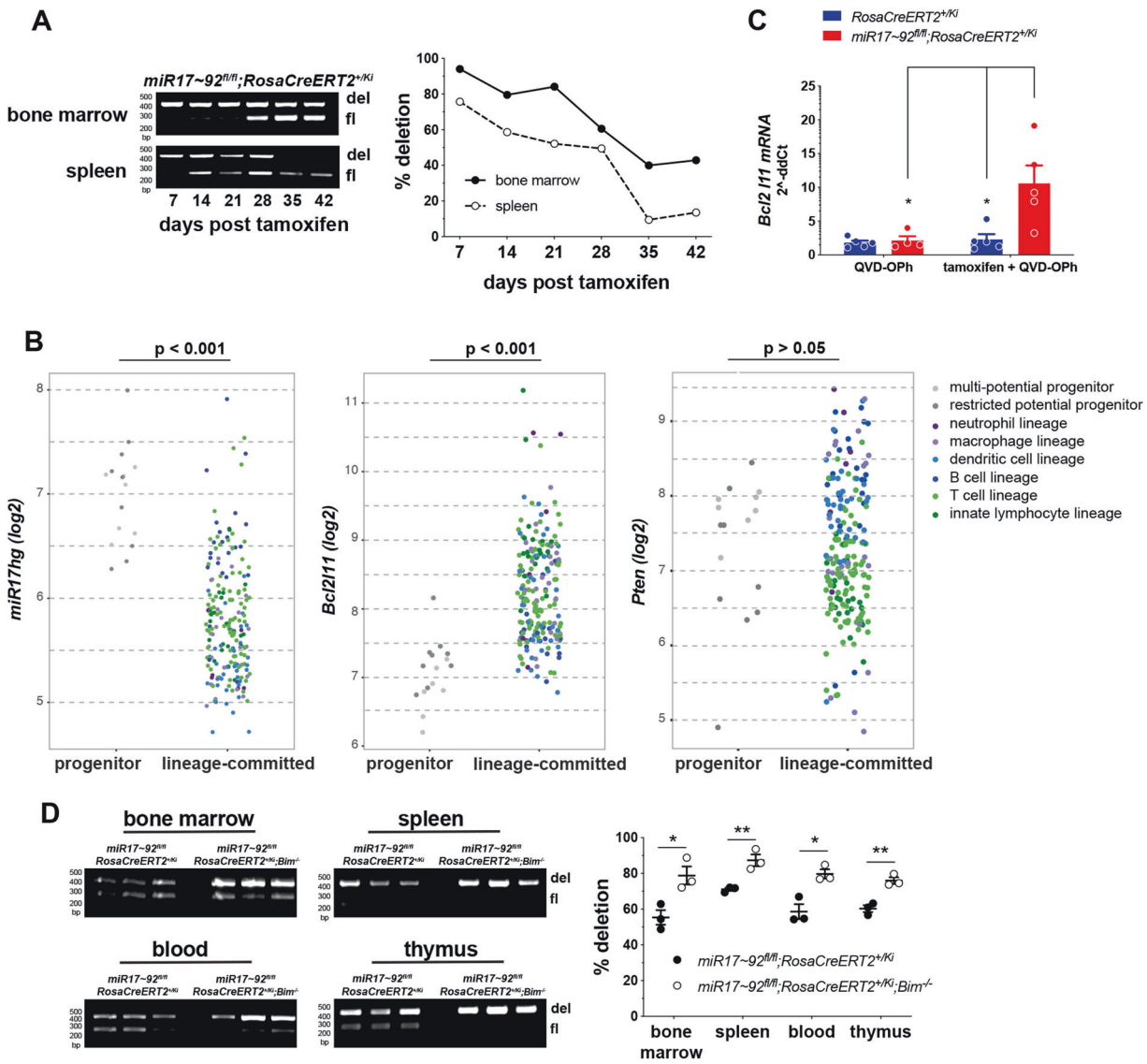

Fig. 1 Induced deletion of *miR17~92* in adult mice leads to BIM dependent loss of diverse haematopoietic cell subsets. **a** Genotyping to detect *miR17~92* wt, floxed and del bands of bone marrow (top left) and spleen cells (bottom left) from adult *miR17~92*$^{fl/fl}$; *RosaCreERT2*$^{+/Ki}$ mice at the indicated time points after CreERT2 activation by treatment with tamoxifen (left panel). The efficiency of *miR17~92* deletion was calculated by densitometric analysis of the PCR products of the deleted vs. the non-deleted alleles (right panel). **b** Correlation analysis of *mir17hg* (*miR17~92*), *Bcl2l11 (Bim)* and *Pten* RNA expression in the indicated cell types was determined by examination of microarray data provided by immgen.org [28]. Statistical significance of Pearson correlation was assessed for *mir17hg (miR17~92)* and *Bcl2l11 (Bim)* (−0.2305488, *p*-value: 0.0006382) as well as *mir17hg (miR17~92)* and *Pten* (0.16, *p*-value > 0.05). **c** Total bone marrow cells were isolated from *miR17~92*$^{fl/fl}$; *RosaCreERT2*$^{+/Ki}$ and *RosaCreERT2*$^{+/Ki}$ mice and cultured for 24 h on OP9 stromal cells in the presence or absence of QVD-OPh (25 nM) and tamoxifen (10 µM) to induce CreERT2 activation and *miR17~92* deletion. qPCR analysis using Taq-man probes detecting *Bcl2L11 (Bim)* relative to *HMBS* was performed using the ABI700 machine. Data are presented as mean 2^-ddCT ± SEM pooled from two independent experiments with each performed in triplicates. *$p < 0.05$ (Student's *t* test). **d** Genotyping to detect *miR17~92* wt, floxed and del bands in cells from the bone marrow, spleen, blood and thymus of adult *miR17~92*$^{fl/fl}$; *RosaCreERT2*$^{+/Ki}$ ($n = 3$) and *miR17~92*$^{fl/fl}$; *RosaCreERT2*$^{+/Ki}$; *Bim*$^{-/-}$ mice ($n = 3$) 3 months after CreERT2 activation by treatment with tamoxifen (left panel). The efficiency of *miR17~92* deletion was calculated by densitometric analysis of the PCR products of the deleted vs. the non-deleted alleles (right panel) *$p < 0.05$, **$p < 0.01$ (Student's *t* test)

miR17~92 on a BIM-deficient background did not decrease cellular competitiveness, as demonstrated by an equal contribution of *miR17~92*$^{fl/fl}$; *RosaCreERT2*$^{+/Ki}$; *Bim*$^{-/-}$ cells and GFP competitor cells to the lymphoid (Fig. 2a–c), myeloid (Fig. 2d) and erythroid compartments (Fig. 2e and Supplementary Fig. S2F). In fact, the contributions of *miR17~92*$^{fl/fl}$; *RosaCreERT2*$^{+/Ki}$; *Bim*$^{-/-}$ cells to the B lymphoid compartment in the bone marrow as well as the mature B and T cells

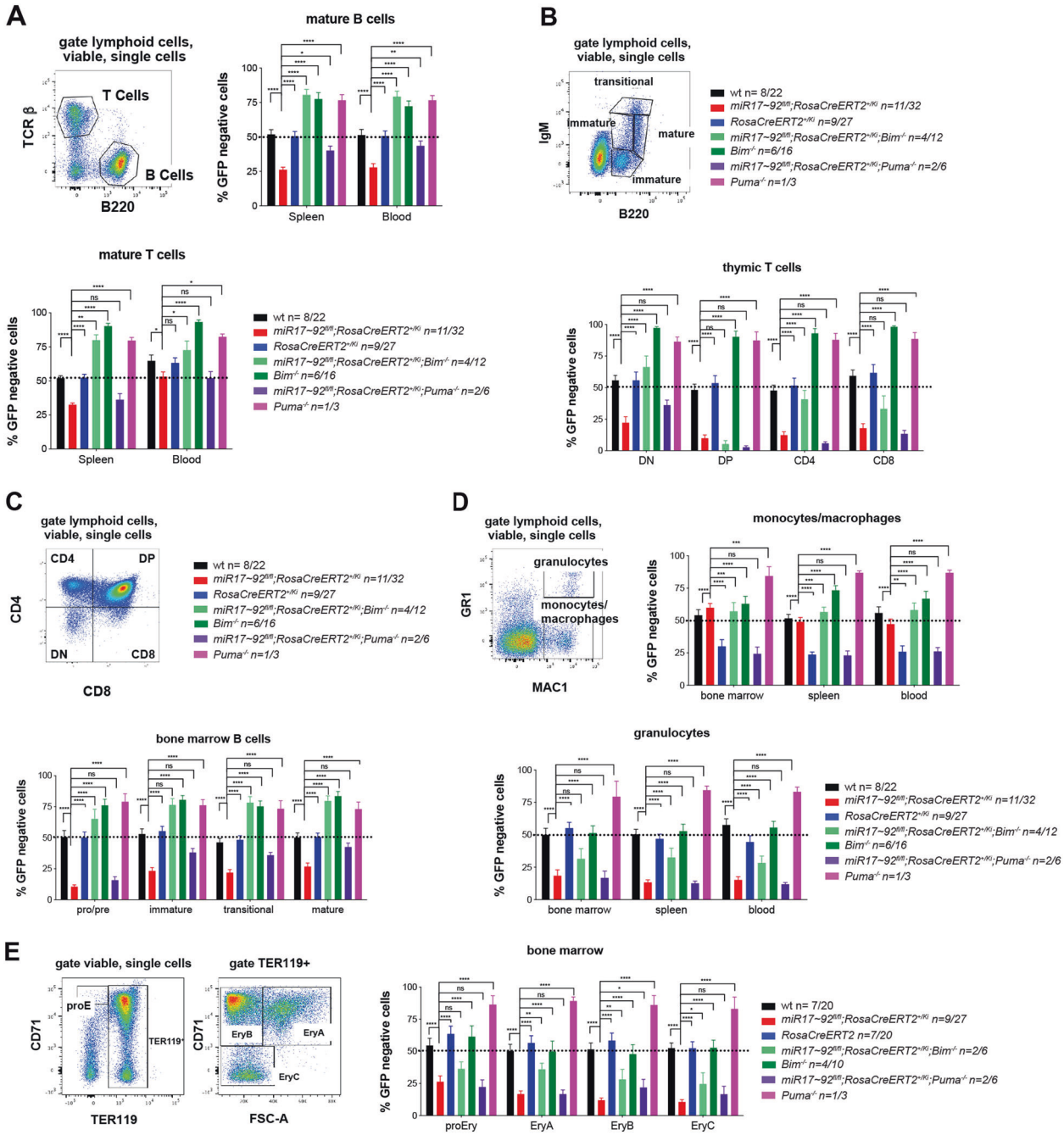

Fig. 2 Loss of BIM rescues haematopoietic cells with deleted *miR17~92*. **a–d** C57BL/6 wt mice (Ly5.1+) were lethally irradiated and reconstituted with a 1:1 mixture of bone marrow cells from UBC-GFP mice (competitor cells) and bone marrow cells from mice of the indicated genotypes (test cells). Reconstituted mice were treated with tamoxifen (three doses oral gavage, 60 mg/kg/day) 8–15 weeks post-transplantation to activate the CreERT2 recombinase. After an additional 8–10 weeks, the immature as well as mature lymphoid and myeloid cell populations were analysed by flow cytometry. **a** Mature B and T cells in the spleen and peripheral blood were identified by staining with antibodies against B220 and TCRβ. **b** Immature and mature thymic T cell populations were identified by staining with antibodies against CD4 and CD8. DN = double negative $CD4^{-}CD8^{-}$; DP = double positive $CD4^{+}CD8^{+}$ cells. **c** Immature and mature B cell populations of the bone marrow were identified by staining with antibodies against B220 and IgM: pro-B/pre-B ($B220^{+}IgM^{-}$), immature B ($B220^{low}IgM^{+}$, transitional B ($B220^{+}IgM^{high}$) and mature B cells ($B220^{high}IgM^{+}$). **d** Monocytes/macrophages ($MAC\text{-}1^{+}GR\text{-}1^{low}$) and granulocytes ($MAC\text{-}1^{+}GR\text{-}1^{high}$) were identified in the bone marrow and spleen by staining with antibodies against MAC-1 and GR-1. **e** Immature and mature erythroid cell populations were identified in the bone marrow by staining with antibodies against TER119 and CD71 as well as by size discrimination using forward light scatter (FSC-A). Ery = erythroid. **a–e** Representative FACS plots for the gating strategies are provided for cells from wt mice. Percentages of GFP-negative cells (test cells) were determined for each cell subset. Data represent mean ± SEM. $*p < 0.05$, $**p < 0.01$, $***p < 0.001$, $****p < 0.0001$ (Student's *t* test *miR17~92*$^{fl/fl}$; *RosaCreERT2*$^{+/Ki}$ vs. wt, *RosaCreERT2*$^{+/Ki}$, *miR17~92*$^{fl/fl}$; *RosaCreERT2*$^{+/Ki}$; *Bim*$^{-/-}$, *Bim*$^{-/-}$, *miR17~92*$^{fl/fl}$; *RosaCreERT2*$^{+/Ki}$; *Puma*$^{-/-}$ and *Puma*$^{-/-}$ mice). *n* = number of donor/number of recipient mice as indicated

in the spleen were significantly >50%. This is consistent with the accumulation of these cell types seen in BIM-deficient mice [15].

We next wanted to validate that the rescue of *miR17~92*-deleted cells by the loss of BIM is not due to a general rescue from apoptosis but due to direct derepression of BIM function. Therefore, we assessed the impact of the absence of PUMA another pro-apoptotic BH3-only protein that also plays critical roles in the haematopoietic system [24, 33, 34], on the reduction of haematopoietic cells caused by the induced deletion of *miR17~92*. In contrast to the *Bim3′UTR*, the *Puma3′UTR* does not harbor putative binding sites for any of the mature members of the *miR17~92* cluster (targetscan.org [35]). While the loss of BIM could rescue most mature and immature haematopoietic cell populations from the consequences of *miR17~92* deletion, loss of PUMA had significant impact on only a subset of these cell populations (Fig. 2). Most effects of PUMA loss were seen in immature and mature B cells, although their rescue from *miR17~92* deletion was still less pronounced than that observed by the absence of BIM (Fig. 2a, c). Collectively, these data demonstrate that the loss of competitiveness of haematopoietic cells caused by the deletion of the *miR17~92* cluster is driven by apoptotic cell death triggered by derepression of the BH3-only protein BIM.

miR17~92 regulates the survival of haematopoietic stem and progenitor cells by restraining BIM-induced apoptosis

The reduction of all haematopoietic cell subsets observed after deletion of *miR17~92* could be due to the independent loss of both immature and mature cell types. Alternatively, it could be a consequence of the loss of common HSPCs causing subsequent reductions in their differentiated progeny. To examine this, we first analysed the fate of HSPCs in competitive haematopoietic reconstitution assays using foetal liver cells from E14.5 $miR17\sim92^{del/del}$, $miR17\sim92^{+/del}$ (*del* = gene deleted in all cells of the embryo) or wt embryos as test cells and foetal liver cells from E14.5 GFP embryos as competitor cells. A significant competitive disadvantage to reconstitute the host haematopoietic system was observed for E14.5 foetal liver cells from $miR17\sim92^{del/del}$ embryos (Fig. 3). Of note, there was almost no contribution observed of the GFP-negative $miR17\sim92^{del/del}$ cells to the lineage$^-$c-KIT$^+$SCA-1$^+$ (LSK), haematopoietic stem/progenitor (Fig. 3a) as well as lineage-committed pluripotent progenitor cells, including common lymphoid progenitors (CLPs), common myeloid progenitors (CMPs), megakaryocyte erythroid progenitors (MEPs) and granulocyte monocyte progenitors (GMPs) (Fig. 3b). In contrast the control donor cells (wt, $miR17\sim92^{+/del}$) contributed at least 50% to these HSPC compartments (Fig. 3a, b). A more detailed analysis of the HSPC populations, using either the stem cell markers of the FLK (foetal liver kinase) series [36] (Fig. 3c) or the SLAM (signalling lymphocytic activation molecule) series [37] (Fig. 3d), revealed that deletion of *miR17~92* greatly reduced the competitiveness of all HSPC subsets.

A significant decrease in the numbers of LSK, HSC and most progenitor cells, including CLPs, CMPs, MEPs and GMPs was also evident in foetal livers from E14.5 $miR17\sim92^{del/del}$ embryos when compared with foetal livers from wt controls (Supplementary Fig. S3). This demonstrates that the loss of *miR17~92* impairs the survival of all HSPC populations in both a transplantation as well as a steady state setting.

To expand on these findings, we again performed competitive bone marrow reconstitution assays and treated reconstituted mice with tamoxifen to delete *miR17~92* in the test cells (strategy depicted in Supplementary Fig. S2A). We found that 2 months after *miR17~92* deletion only a few LSK stem cell-enriched or early progenitors (lineage$^-$c-KIT$^+$SCA-1$^-$) with deleted *miR17~92* cluster were present in the competitive setting (Fig. 4a). A more detailed analysis of the HSPC populations, using either the stem cell markers of the SLAM series [37] (Fig. 4b) or the FLK series markers [36] (Fig. 4c), revealed that deletion of *miR17~92* did not substantially affect the long-term (LT)-HSCs but greatly diminished the competitiveness of the early HSPCs with self-renewal capacity, such as short-term (ST)-HSCs and multipotent progenitors (MPPs). In all of these tests, oligopotent progenitors (Fig. 5a) as well as early lineage-committed progenitors of the myeloid (pre-GMs and GMs), erythroid (pre-CFU-E, CFU-E) and megakaryocyte lineages (MegE, MK) were significantly disadvantaged upon deletion of *miR17~92* (Fig. 5a–c). In striking contrast, $miR17\sim92^{fl/fl}$; $RosaCreERT2^{+/Ki}$; $Bim^{-/-}$ donor cells were able to contribute efficiently to all HSPC subsets (Figs. 4 and 5). In fact, the $miR17\sim92^{fl/fl}$; $RosaCreERT2^{+/Ki}$; $Bim^{-/-}$ donor cells contributed significantly >50% to several of these compartments. Importantly, $miR17\sim92^{fl/fl}$; $RosaCreERT2^{+/Ki}$; $Puma^{-/-}$ donor cells did not contribute more than the $miR17\sim92^{fl/fl}$; $RosaCreERT2^{+/Ki}$ donor cells to the LSK and progenitor compartments (Fig. 4a). This reveals that BIM, but not PUMA, is the critical initiator of apoptosis targeted by the *miR17~92* cluster in HSPCs. Interestingly, in multipotent progenitor cells the loss of PUMA could alleviate the lack of competitiveness caused by the deletion of the *miR17~92* cluster. However, this protection was still less pronounced than that observed by the loss of BIM (Fig. 4c). These findings further demonstrate that HSPCs rely for their survival on *miR17~92*-mediated suppression of apoptotic death mainly via direct suppression of the pro-apoptotic BH3-only protein BIM.

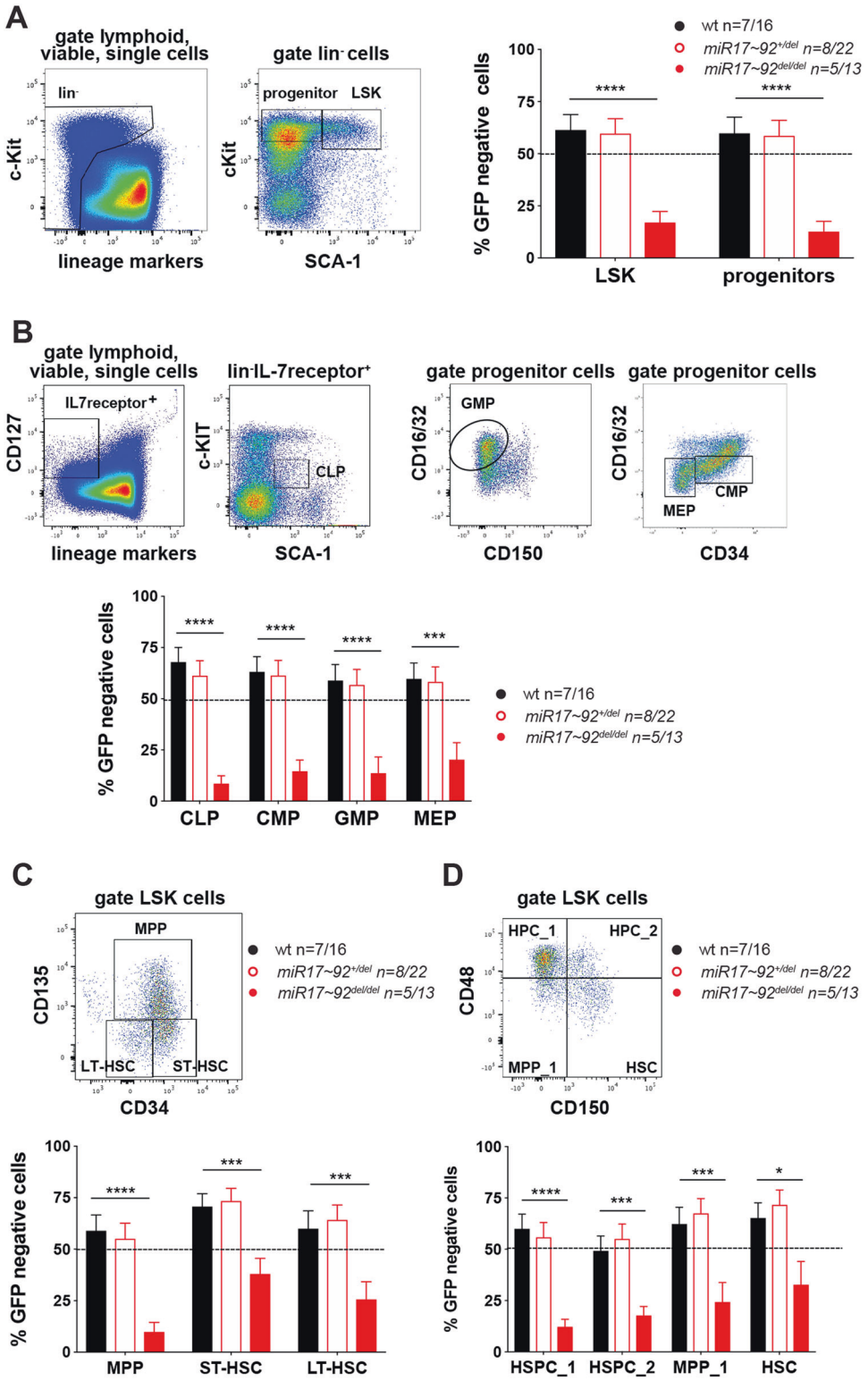
A
gate lymphoid, viable, single cells
lin-
c-Kit
lineage markers
gate lin- cells
progenitor LSK
cKit
SCA-1
wt n=7/16
miR17~92+/del n=8/22
miR17~92del/del n=5/13
% GFP negative cells
****
****
LSK
progenitors
B
gate lymphoid, viable, single cells
IL7receptor+
CD127
lineage markers
lin-IL-7receptor+
c-KIT
CLP
SCA-1
gate progenitor cells
GMP
CD16/32
CD150
gate progenitor cells
CD16/32
CMP
MEP
CD34
% GFP negative cells
****
****
****
***
CLP
CMP
GMP
MEP
wt n=7/16
miR17~92+/del n=8/22
miR17~92del/del n=5/13
C
gate LSK cells
MPP
CD135
LT-HSC
ST-HSC
CD34
wt n=7/16
miR17~92+/del n=8/22
miR17~92del/del n=5/13
% GFP negative cells
****
***
***
MPP
ST-HSC
LT-HSC
D
gate LSK cells
HPC_1
HPC_2
CD48
MPP_1
HSC
CD150
wt n=7/16
miR17~92+/del n=8/22
miR17~92del/del n=5/13
% GFP negative cells
****
***
***
*
HSPC_1
HSPC_2
MPP_1
HSC

◀ **Fig. 3** Induced deletion of the *miR17~92* cluster causes a loss of haematopoietic stem and progenitor cells (HSPCs). C57BL/6 wt mice (Ly5.1+) were lethally irradiated and reconstituted with a 1:1 mixture of E14.5 foetal liver cells from UBC-GFP embryos (competitor cells) and E14.5 foetal liver cells from *miR17~92*^{deldel}, *miR17~92*$^{+/del}$ or wt embryos (test cells). At 8–10 weeks after transplantation, the fraction of reconstituted test cells was determined by FACS analysis gating on Ly5.1^{+}GFP^{-} cells (donor test cells). Representative FACS plots for the gating strategies are provided for wt mice. Percentages of GFP-negative cells (test cells) were determined for the indicated cell populations. Data represent mean ± SEM. *$p < 0.05$, **$p < 0.01$, ***$p < 0.001$, ****$p < 0.0001$ (Student's *t* test *miR17~92*^{deldel}, *miR17~92*$^{+/del}$ and wt). **a** LSK (lineage^{-}c-KIT^{+}SCA-1^{+}) cells and progenitor cells (lineage^{-}c-KIT^{+}SCA-1^{-}) were identified in the lineage marker negative compartment (TER119^{-}, CD4^{-}, CD8a^{-}, Ly6G^{-}, B220^{-}, CD2^{-}, CD3^{-}, CD19^{-}, F4/80^{-}, NK1.1^{-}, GR-1^{-}) by staining with antibodies against c-KIT and SCA-1. **b** Oligopotent progenitors, including common myeloid progenitors (CMP), granulocyte/macrophage progenitors (GMP) and megakaryocyte/erythroid progenitors, were identified by cell surface staining for the SLAM markers (CD16/32, CD150, CD34) in the progenitor cell population (lineage^{-}c-KIT^{+}SCA-1^{-}). Common lymphoid progenitors (CLP) were identified as c-KIT^{med}SCA-1^{med}IL-7 receptor^{+} within the lineage marker negative cell populations. **c** Long-term haematopoietic stem cells (LT-HSC), short-term haematopoietic stem cells (ST-HSC) as well as multipotent progenitor cells (MPP) were identified using the FLK series markers (CD34, CD135) within the LSK cell population. **d** Haematopoietic stem cells (HSC), multipotent progenitor cells (MPP) and haematopoietic progenitor cells (HPC-1/2) were identified using cell surface staining for the SLAM markers (CD48, CD150) within the LSK cell population. *n* = number of donor/number of recipient mice as indicated

miR17~92 is critical for the survival of human CD34^{+} haematopoietic stem/progenitor cells by restraining BIM-induced apoptosis

Our study identified the importance of *miR17~92*-mediated suppression of BIM-induced apoptosis for the survival of murine HSPCs. To extend our studies into the human system, we tested whether *miR17~92*-mediated suppression of *BIM* expression also plays a critical role in human HSPCs. To this end we assessed the colony forming capacity of human CD34^{+} cells from cord blood in the absence or presence of MIR17PTi, a recently described specific inhibitor of *pri-miR17~92* [29]. Remarkably, the colony forming capacity of human CD34^{+} cells derived from two individual donors was reduced in the presence of the MIR17PTi, whereas no impact was observed when colony formation was assessed in the presence of a non-targeting (scrambled) oligo (Fig. 6a).

To investigate the direct interaction of individual mature miRNAs of the *miR17~92* cluster with the human *BIM* mRNA, we exploited *miR17~92* target protectors, which specifically block the binding of *miR17~92* family members to specific sites in the *3′UTR* of the *BIM* mRNA. The *BIM 3′UTR* harbors at least four potential binding sites, including *miR17*, *miR19* and *miR92* seed family sequences [5]. Human CD34^{+} cells were transfected with four individual target protectors covering the four highly conserved predicted binding sites for mature miRNAs of the *miR17~92* cluster. Remarkably, CD34^{+} cells from four of the five human donors underwent apoptotic cell death upon transfection with the aforementioned target protectors, with the most prominent effect observed in response to the *miR19 or miR92* target protectors (Fig. 6b). These results demonstrate that *miR17~92*-mediated suppression of BIM-induced apoptosis is also crucial for the survival of human HSPCs.

Discussion

The *miR17~92* cluster has been shown to play a critical role in the survival of immature as well as mature B lymphoid cells [7]. Our present study reveals a previously unknown pro-survival function of the *miR17~92* cluster in HSPCs. Remarkably, amongst the many predicted targets reported to be bound and suppressed by the *miR17~92* cluster, *Bim* appears to be the most important, given that the mere loss of this pro-apoptotic BH3-only protein fully prevented all defects caused by the deletion of *miR17~92*.

While the conditional deletion of *miR17~92* in adult mice did not impact the LT-HSCs, all subsequent stages, including the ST-HSC, MPP and lineage-committed progenitors, were found to depend on *miR17~92*-mediated suppression of BIM-induced apoptosis for their survival. Notably, loss of PUMA, another highly potent pro-apoptotic BH3-only protein [38, 39], could rescue the survival defect caused by the deletion of *miR17*~92 only in a subset of haematopoietic cell populations, including MPPs and B cells, and to a considerably lesser extent compared with the loss of BIM. This partial rescue afforded by the absence of PUMA in some haematopoietic cell subsets is consistent with the observation that BIM and PUMA have overlapping functions in developmentally programmed as well as cytotoxic stress-induced death of lymphoid cells [40]. Why does loss of PUMA show any protection when *miR17~92* is deleted? The most likely explanation is that the absence of PUMA frees up pro-survival BCL-2 family members in the cells that are then capable of neutralising BIM. Hence, deletion of *miR17~92* causes an increase in the levels of BIM, which can be more efficiently neutralised by BCL-2, MCL-1 and their relatives when PUMA is deleted as more such free pro-survival proteins are available. Remarkably, even though *Puma*$^{-/-}$ cells had a survival advantage over wt cells (without deletion of *miR17~92*) in almost all haematopoietic cell subsets tested, loss of PUMA was not sufficient to rescue the survival defects induced by the deletion of the *miR17~92* cluster in most of these cell populations. Of note loss of BIM on a wt background resulted in a survival advantage of several

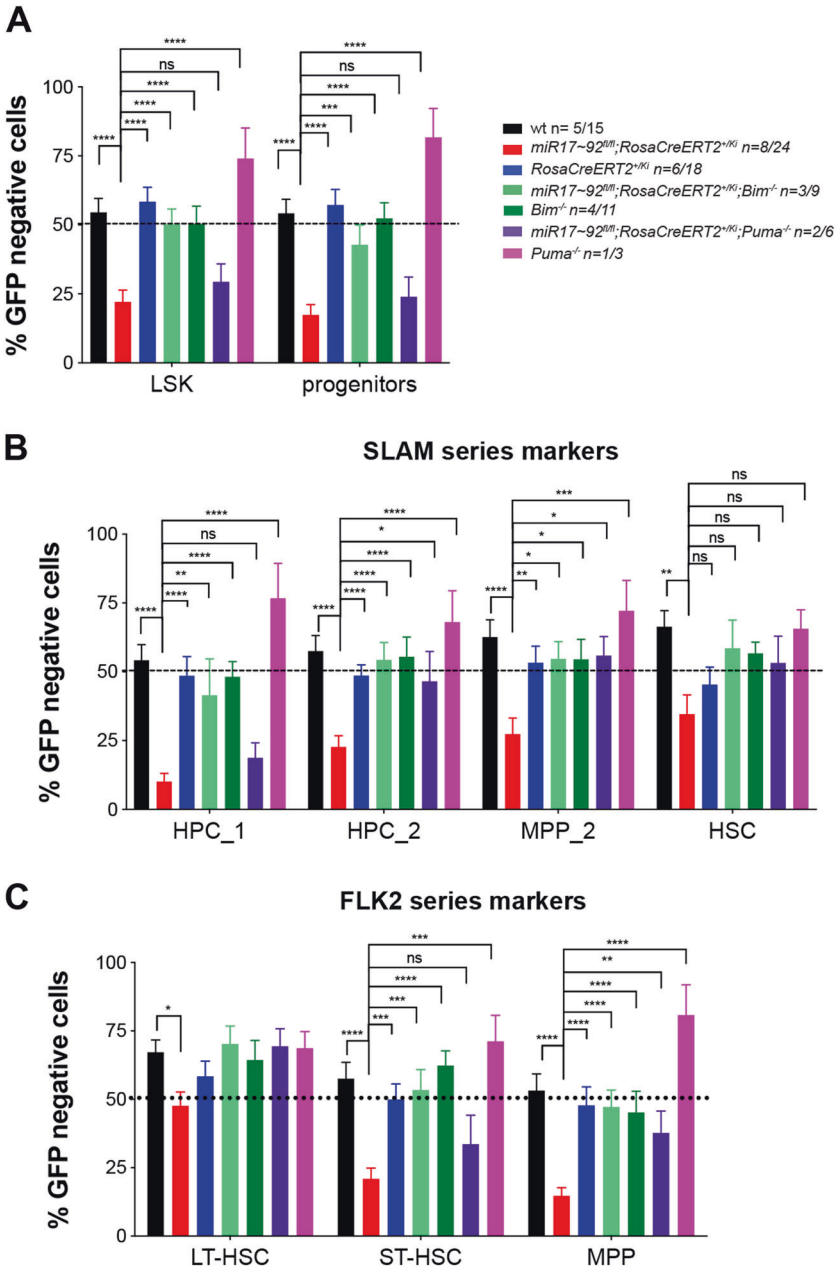

Fig. 4 The reduction of haematopoietic stem and progenitor cells (HSPCs) caused by the induced deletion of *miR17~92* can be fully prevented by the loss of pro-apoptotic BIM. **a–c** C57BL/6 wt mice (Ly5.1+) were lethally irradiated and reconstituted with a 1:1 mixture of bone marrow cells from UBC-GFP mice (competitor cells) and bone marrow cells from mice of the indicated genotypes (test cells). Reconstituted mice were treated with tamoxifen 8–15 weeks post-transplantation to activate the CreERT2 recombinase. After an additional 8–10 weeks the haematopoietic stem/progenitor cell populations (HSPC) indicated were identified by staining with antibodies against cell type specific surface markers. Representative FACS plots for the gating strategies are provided for wt mice in Fig. 3. Percentages of GFP-negative cells (test cells) were determined for each cell subset. Data represent mean ± SEM. $*p < 0.05$, $**p < 0.01$, $***p < 0.001$, $****p < 0.0001$ (Student's *t* test *miR17~92*$^{fl/fl}$; *RosaCreERT2*$^{+/Ki}$ vs. wt, *RosaCreERT2*$^{+/Ki}$, *miR17~92*$^{fl/fl}$; *RosaCreERT2*$^{+/Ki}$; *Bim*$^{-/-}$, *Bim*$^{-/-}$, *miR17~92*$^{fl/fl}$; *RosaCreERT2*$^{+/Ki}$; *Puma*$^{-/-}$ and *Puma*$^{-/-}$ mice). *n* = number of donor/number of recipient mice as indicated

mature haematopoietic cell subsets but not HSPCs or immature cells of the lymphoid and erythroid lineage in the bone marrow (Figs. 2, 4). This is in line with the notion that *miR17~92* is highly expressed in HSPCs (Fig. 1b), thereby capable of repressing *Bim mRNA* effectively in these cell populations. These high levels of *miR17~92* result in low expression of BIM, which is similar to the loss of BIM by genetic deletion. Therefore, it would be expected that the genetic loss of *Bim* in *miR17~92* high-expressing cells has no or only little impact on their survival, because this microRNA cluster already efficiently restrains the expression of this initiator of apoptosis.

Our studies with human CD34$^+$ HSPCs treated with a specific inhibitor of *pri-miR17~92* (MIR17PTi) [29] confirmed the critical role of *miR17~92*-mediated repression of *BIM* for their survival given that this reagent substantially reduced the haematopoietic colony forming potential of these cells. Accordingly, the expression of microRNA target protectors (mirScript) designed to bind to four specific regions in the *BIM 3′UTR* [5] in human CD34$^+$ cells induced marked apoptotic cell death. Interestingly, we observed apoptotic cell death upon targeting of several *miR17~92* seed-match sequences in the human *BIM* 3′UTR. However, one out of five human CD34$^+$ HSPC samples did

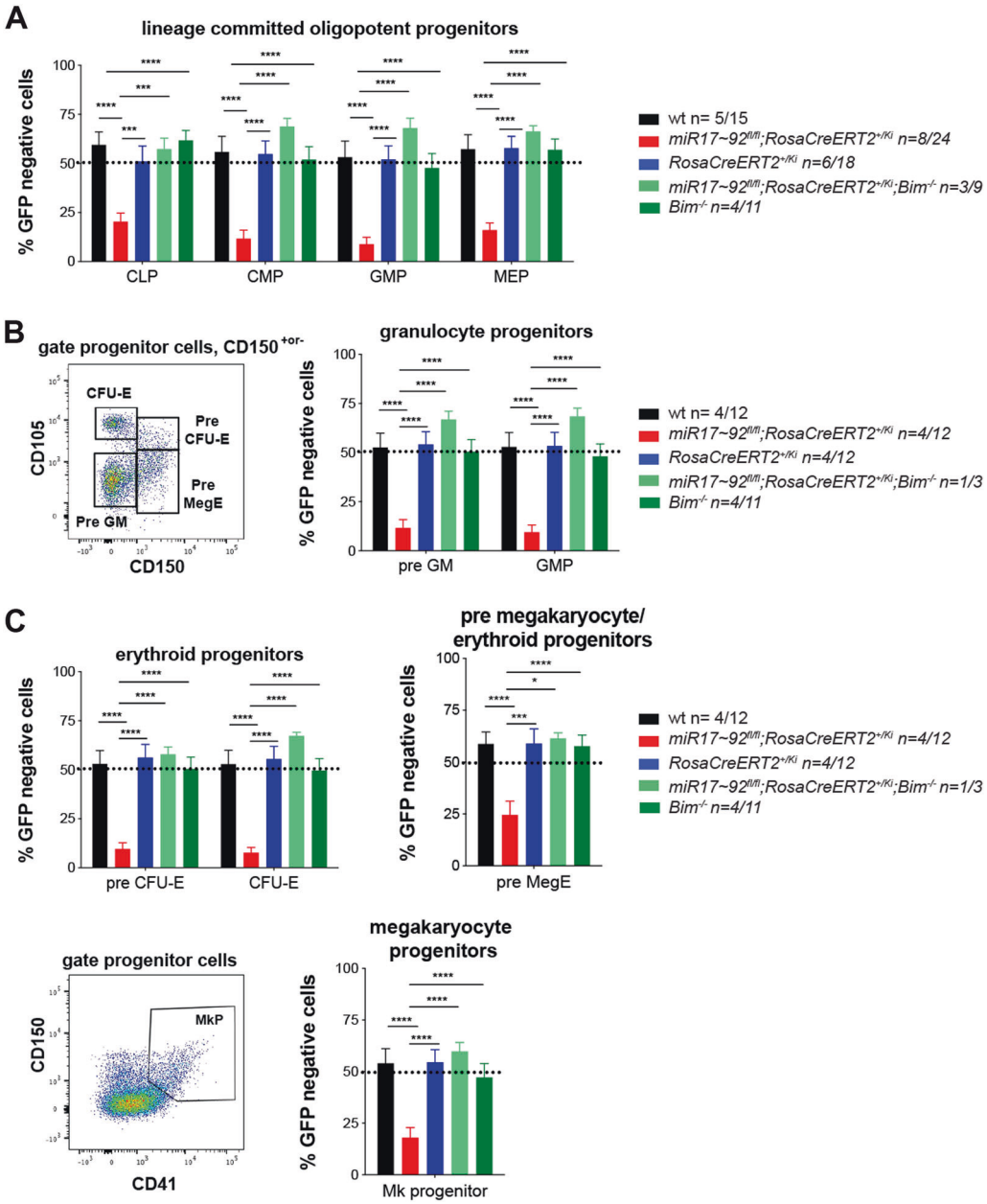

Fig. 5 The induced deletion of *miR17~92* causes a substantial reduction in lineage-committed haematopoietic progenitor cells and this can be completely prevented by the concomitant loss of BIM. C57BL/6 wt mice (Ly5.1+) were lethally irradiated and reconstituted with a 1:1 mixture of bone marrow cells from UBC-GFP mice (competitor cells) and bone marrow cells from mice of the indicated genotypes (test cells). Reconstituted mice were treated with tamoxifen 8–10 weeks post-transplantation to activate the CreERT2 recombinase. After an additional 8–10 weeks, the haematopoietic progenitor cell populations were identified by staining with antibodies against cell type specific surface markers as indicated in the representative FACS plots. The percentages of GFP-negative cells (test cells) were determined for the indicated cell populations. Data represent mean ± SEM. $*p < 0.05$, $**p < 0.01$, $***p < 0.001$, $****p < 0.0001$ (Student's *t* test *miR17~92*$^{fl/fl}$; *RosaCreERT2*$^{+/Ki}$ vs. wt, *RosaCreERT2*$^{+/Ki}$, *miR17~92*$^{fl/fl}$; *RosaCreERT2*$^{+/Ki}$; *Bim*$^{-/-}$ and *Bim*$^{-/-}$ mice). Representative FACS plots indicating the gating strategy and staining for the cell surface markers used are provided for wt mice. **a** Lineage-committed progenitor cells, including CLP (common lymphoid progenitor), CMP (common myeloid progenitor), GMP (granulocyte/macrophage progenitor) and MEP (megakaryocyte/erythroid progenitor) populations, **b** granulocyte progenitors, including the pre-GM and GM cell populations, and **c** pre-megakaryocyte/erythroid progenitors (Pre-MegE), megakaryocyte (MK progenitors) and the erythroid progenitors, pre-CFU-E (colony forming unit erythroid) and CFU-E were examined in the competitive haematopoietic reconstitution assay using staining for the indicated markers

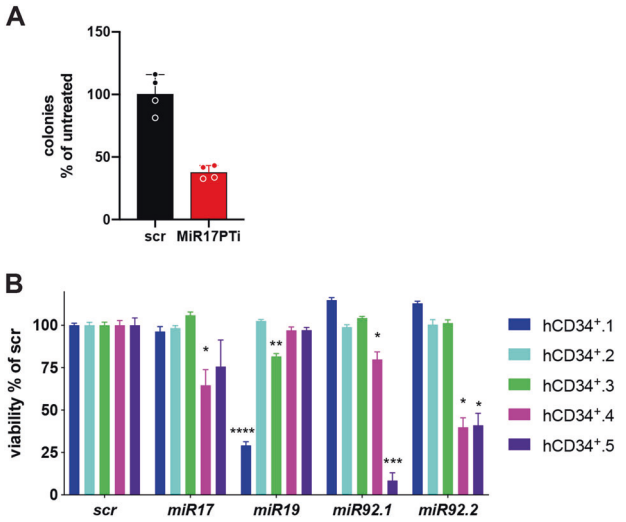

Fig. 6 m*iR17~92* is critical for the survival of human CD34$^+$ haematopoietic stem/progenitor cells (HSPCs) by restraining BIM-induced apoptosis. **a** Human CD34$^+$ cord blood cells where cultured with 20 µM MIR17PTi [29] or scrambled control (scr) and the total numbers of colonies were counted and calculated as relative to no drug treated samples. Data are presented as mean ± SEM from two human CD34$^+$ cord blood cell samples, each tested in duplicates. *$p < 0.05$, **$p < 0.01$, ***$p < 0.001$, ****$p < 0.0001$. **b** human CD34$^+$ cord blood cells ($n = 5$) were transfected in triplicates with the indicated mirScript target protectors (Qiagen) together with a reporter plasmid encoding for GFP. At 48 h after transfection the cell viability of the transfected (GFP$^+$) cells was assessed by flow cytometric analysis upon staining with AnnexinV-647 and DAPI with viable cells defined as AnnexinV negative/DAPI negative. Data (normalised to scrambled (scr) control samples) are presented as mean ± SEM. *$p < 0.05$, **$p < 0.01$, ***$p < 0.001$, ****$p < 0.0001$ (Student's *t* test comparing individual target protectors to the scr control)

not respond to any of the target protectors. It is tempting to speculate, that polymorphisms in the *miR17~92* seed regions of the *BIM* 3′UTR in this donor may be responsible for the observed resistance. So how could BIM be kept in check in such a scenario? One could imagine that positive regulators of gene expression that act on the *BIM* 3′UTR are downregulated to allow less dependence on *miR17~92*-mediated repression of BIM, but further studies are required to confirm this hypothesis.

While several in silico and in vitro findings provided evidence for the regulation of BIM expression through its 3′ UTR by the *miR17~92* cluster [5, 6, 22, 29, 41, 42], functional demonstration that BIM is regulated in physiological settings in vivo by such a process has never been reported before. This makes the post-transcriptional regulation of *Bim* by *miR17~92* thus far the only in vivo validated regulatory mechanism of BIM expression, given that the importance of previously in vitro reported transcriptional (FOXO transcription factors) and post-translational (ERK-mediated phosphorylation) processes for regulating BIM expression could not be confirmed in physiological settings within the context of a whole organism [43, 44].

In conclusion, our studies reveal that *miR17~92* plays a critical role in the survival of both mouse and human HSPCs and committed progenitors by restraining the expression of pro-apoptotic BIM. Moreover, our results uncover for the first time a regulatory mechanism of BIM that is important in the context of haematopoietic cell survival and development within the whole organism. The observation that the mere absence of BIM is capable to completely prevent all defects caused by the deletion of the *miR17~92* cluster is a remarkable finding as many targets bound and suppressed by this microRNA cluster have been reported with their repression proposed to be critical for normal physiology. Based on our findings, it is tempting to speculate that microRNA functions in the context of a whole organism might be less complex than previously assumed and this could be uncovered by more in vivo experimentation through comparing the impact of the absence of a microRNA cluster with the phenotype of the combined absence of this microRNA cluster and one of its targets at the same time.

Acknowledgements We thank C Stivala, S Russo, J Mansheim, T Baldinger, M Patsis and G Siciliano for expert animal care; B Helbert and K Mackwell for genotyping; J Corbin and J McManus for automated blood analysis; S Monard and his team for help with flow cytometry; S Mifsud for assistance with colony assays and Dr P Bouillet for providing *Bim*$^{-/-}$ mice. This work was supported by grants and fellowships from the Deutsche Krebshilfe (Dr Mildred Scheel post-doctoral fellowship to KB) the Australian National Health and Medical Research Council (NHMRC) (Project Grants 1145728 to MJH, 1143105 to MJH and AS, 1122783 to APN, Program Grants 1016701 to AS and 1113577 to WSA and Fellowships 1020363 to AS, 1058344 to WSA, 1156095 to MJH, GNT1035229 to CAdG and 1124788 to NDH), the Leukemia and Lymphoma Society of America (LLS SCOR 7001-13 to AS and MJH), the Cancer Council of Victoria (project grant 1052309 to AS and Venture Grant to MJH and AS), a Victorian Cancer Agency Fellowship (ECSG18020 to JR) as well as by operational infrastructure grants through the Australian Government Independent Research Institute Infrastructure Support Scheme (361646 and 9000220) and the Victorian State Government Operational Infrastructure Support Program.

Author contributions KB, MJH and AS designed and conceived the study, planned experiments and prepared the paper. KB conducted and analysed the experiments. CAdG helped with the analysis of the RNA expression data (Fig. 1b) CH and WSA provided advice for the analysis of the LT-HSC compartment, helped with these experiments and data analysis and provided the antibodies for staining cells (Figs. 3–5). APN and LDR performed the colony formation assays (Fig. 6a). JR and NDH gave advice on experiments with human CD34$^+$ cord blood cells and provided the cells and media (Fig. 6). EM provided MIR17PTi and helped with planning the colony formation assays (Fig. 6a).

Compliance with ethical standards

Conflict of interest The authors declare that they have no conflict of interest.

References

1. Bartel DP. MicroRNAs: genomics, biogenesis, mechanism, and function. Cell. 2004;116:281–97.
2. Lewis BP, Shih IH, Jones-Rhoades MW, Bartel DP, Burge CB. Prediction of mammalian microRNA targets. Cell. 2003;115:787–98.
3. Tanzer A, Stadler PF. Molecular evolution of a microRNA cluster. J Mol Biol. 2004;339:327–35.
4. Lu Y, Thomson JM, Wong HY, Hammond SM, Hogan BL. Transgenic over-expression of the microRNA miR-17-92 cluster promotes proliferation and inhibits differentiation of lung epithelial progenitor cells. Dev Biol. 2007;310:442–53.
5. Ventura A, Young AG, Winslow MM, Lintault L, Meissner A, Erkeland SJ, et al. Targeted deletion reveals essential and overlapping functions of the miR-17 through 92 family of miRNA clusters. Cell. 2008;132:875–86.
6. Xiao C, Srinivasan L, Calado DP, Patterson HC, Zhang B, Wang J, et al. Lymphoproliferative disease and autoimmunity in mice with increased miR-17-92 expression in lymphocytes. Nat Immunol. 2008;9:405–14.
7. Jiang S, Li C, Olive V, Lykken E, Feng F, Sevilla J, et al. Molecular dissection of the miR-17-92 cluster's critical dual roles in promoting Th1 responses and preventing inducible Treg differentiation. Blood. 2011;118:5487–97.
8. Shan SW, Lee DY, Deng Z, Shatseva T, Jeyapalan Z, Du WW, et al. MicroRNA MiR-17 retards tissue growth and represses fibronectin expression. Nat Cell Biol. 2009;11:1031–8.
9. Chamorro-Jorganes A, Lee MY, Araldi E, Landskroner-Eiger S, Fernandez-Fuertes M, Sahraei M, et al. VEGF-induced expression of miR-17-92 cluster in endothelial cells is mediated by ERK/ELK1 activation and regulates angiogenesis. Circ Res. 2016;118:38–47.
10. Landskroner-Eiger S, Qiu C, Perrotta P, Siragusa M, Lee MY, Ulrich V, et al. Endothelial miR-17 approximately 92 cluster negatively regulates arteriogenesis via miRNA-19 repression of WNT signaling. Proc Natl Acad Sci USA. 2015;112:12812–7.
11. Lau KW, Stiffel VM, Rundle CH, Amoui M, Tapia J, White TD, et al. Conditional disruption of miR17~92 in osteoclasts led to activation of osteoclasts and loss of trabecular bone in part through suppression of the miR17-mediated downregulation of protein-tyrosine phosphatase-oc in mice. JBMR. 2017;1:73–85.
12. Bian S, Hong J, Li Q, Schebelle L, Pollock A, Knauss JL, et al. MicroRNA cluster miR-17-92 regulates neural stem cell expansion and transition to intermediate progenitors in the developing mouse neocortex. Cell Rep. 2013;3:1398–406.
13. de Pontual L, Yao E, Callier P, Faivre L, Drouin V, Cariou S, et al. Germline deletion of the miR-17 approximately 92 cluster causes skeletal and growth defects in humans. Nat Genet. 2011;43:1026–30.
14. Regelin M, Blume J, Pommerencke J, Vakilzadeh R, Witzlau K, Lyszkiewicz M, et al. Responsiveness of developing T cells to IL-7 signals is sustained by miR-17 approximately 92. J Immunol. 2015;195:4832–40.
15. Bouillet P, Metcalf D, Huang DC, Tarlinton DM, Kay TW, Kontgen F, et al. Proapoptotic Bcl-2 relative Bim required for certain apoptotic responses, leukocyte homeostasis, and to preclude autoimmunity. Science. 1999;286:1735–8.
16. Strasser A, Whittingham S, Vaux DL, Bath ML, Adams JM, Cory S, et al. Enforced BCL2 expression in B-lymphoid cells prolongs antibody responses and elicits autoimmune disease. Proc Natl Acad Sci USA. 1991;88:8661–5.
17. McDonnell TJ, Deane N, Platt FM, Nunez G, Jaeger U, McKearn JP, et al. bcl-2-immunoglobulin transgenic mice demonstrate extended B cell survival and follicular lymphoproliferation. Cell. 1989;57:79–88.
18. Han YC, Vidigal JA, Mu P, Yao E, Singh I, Gonzalez AJ, et al. An allelic series of miR-17 approximately 92-mutant mice uncovers functional specialization and cooperation among members of a microRNA polycistron. Nat Genet. 2015;47:766–75.
19. He L, Thomson JM, Hemann MT, Hernando-Monge E, Mu D, Goodson S, et al. A microRNA polycistron as a potential human oncogene. Nature. 2005;435:828–33.
20. Mu P, Han YC, Betel D, Yao E, Squatrito M, Ogrodowski P, et al. Genetic dissection of the miR-17~92 cluster of microRNAs in Myc-induced B-cell lymphomas. Genes Dev. 2009;23:2806–11.
21. Olive V, Bennett MJ, Walker JC, Ma C, Jiang I, Cordon-Cardo C, et al. miR-19 is a key oncogenic component of mir-17-92. Genes Dev. 2009;23:2839–49.
22. Li Y, Choi PS, Casey SC, Dill DL, Felsher DW. MYC through miR-17-92 suppresses specific target genes to maintain survival, autonomous proliferation, and a neoplastic state. Cancer Cell. 2014;26:262–72.
23. Seibler J, Zevnik B, Kuter-Luks B, Andreas S, Kern H, Hennek T, et al. Rapid generation of inducible mouse mutants. Nucleic Acids Res. 2003;31:e12.
24. Villunger A, Michalak EM, Coultas L, Mullauer F, Bock G, Ausserlechner MJ, et al. p53- and drug-induced apoptotic responses mediated by BH3-only proteins puma and noxa. Science. 2003;302:1036–8.
25. Anastassiadis K, Glaser S, Kranz A, Berhardt K, Stewart AF. A practical summary of site-specific recombination, conditional mutagenesis, and tamoxifen induction of CreERT2. Methods Enzymol. 2010;477:109–23.
26. Brinkmann K, Grabow S, Hyland CD, Teh CE, Alexander WS, Herold MJ, et al. The combination of reduced MCL-1 and standard chemotherapeutics is tolerable in mice. Cell Death Differ. 2017;24:2032–43.
27. Pronk CJ, Rossi DJ, Mansson R, Attema JL, Norddahl GL, Chan CK, et al. Elucidation of the phenotypic, functional, and molecular topography of a myeloerythroid progenitor cell hierarchy. Cell Stem Cell. 2007;1:428–42.
28. Heng TS, Painter MW, Immunological Genome Project C. The Immunological Genome Project: networks of gene expression in immune cells. Nat Immunol. 2008;9:1091–4.
29. Morelli E, Biamonte L, Federico C, Amodio N, Di Martino MT, Gallo Cantafio ME, et al. Therapeutic vulnerability of multiple myeloma to MIR17PTi, a first-in-class inhibitor of pri-mir-17-92. Blood. 2018;132:1050–63.
30. Mi S, Li Z, Chen P, He C, Cao D, Elkahloun A, et al. Aberrant overexpression and function of the miR-17-92 cluster in MLL-rearranged acute leukemia. Proc Natl Acad Sci USA. 2010;107:3710–5.
31. de Graaf CA, Choi J, Baldwin TM, Bolden JE, Fairfax KA, Robinson AJ, et al. Haemopedia: an expression atlas of murine hematopoietic cells. Stem Cell Rep. 2016;7:571–82.
32. Choi J, Baldwin TM, Wong M, Bolden JE, Fairfax KA, Lucas EC, et al. Haemopedia RNA-seq: a database of gene expression during haematopoiesis in mice and humans. Nucleic Acids Res. 2019;47(D1):D780–D785.
33. Michalak EM, Jansen ES, Happo L, Cragg MS, Tai L, Smyth GK, et al. Puma and to a lesser extent Noxa are suppressors of Myc-induced lymphomagenesis. Cell Death Differ. 2009;16:684–96.
34. Michalak EM, Villunger A, Adams JM, Strasser A. In several cell types tumour suppressor p53 induces apoptosis largely via Puma but Noxa can contribute. Cell Death Differ. 2008;15:1019–29.

35. Agarwal V, Bell GW, Nam JW, Bartel DP. Predicting effective microRNA target sites in mammalian mRNAs. eLife. 2015;4:05005.
36. Christensen JL, Weissman IL. Flk-2 is a marker in hematopoietic stem cell differentiation: a simple method to isolate long-term stem cells. Proc Natl Acad Sci USA. 2001;98:14541–6.
37. Oguro H, Ding L, Morrison SJ. SLAM family markers resolve functionally distinct subpopulations of hematopoietic stem cells and multipotent progenitors. Cell Stem Cell. 2013;13:102–16.
38. Nakano K, Vousden KH. PUMA, a novel proapoptotic gene, is induced by p53. Mol Cell. 2001;7:683–94.
39. Yu J, Zhang L, Hwang PM, Kinzler KW, Vogelstein B. PUMA induces the rapid apoptosis of colorectal cancer cells. Mol Cell. 2001;7:673–82.
40. Erlacher M, Michalak EM, Kelly PN, Labi V, Niederegger H, Coultas L, et al. BH3-only proteins Puma and Bim are rate-limiting for gamma-radiation- and glucocorticoid-induced apoptosis of lymphoid cells in vivo. Blood. 2005;106:4131–8.
41. Guo Z, Mu X, Ouyang H, Cheng Z, Wang Z, Xu B. Operative treatment of huge adult frontal nasoethmoid meningoencephalocele. J Craniofac Surg. 2013;24:1669–70.
42. Xu Z, Sharp PP, Yao Y, Segal D, Ang CH, Khaw SL, et al. BET inhibition represses miR17-92 to drive BIM-initiated apoptosis of normal and transformed hematopoietic cells. Leukemia. 2016;30:1531–41.
43. Clybouw C, Merino D, Nebl T, Masson F, Robati M, O'Reilly L, et al. Alternative splicing of Bim and Erk-mediated Bim(EL) phosphorylation are dispensable for hematopoietic homeostasis in vivo. Cell Death Differ. 2012;19:1060–8.
44. Herold MJ, Rohrbeck L, Lang MJ, Grumont R, Gerondakis S, Tai L, et al. Foxo-mediated Bim transcription is dispensable for the apoptosis of hematopoietic cells that is mediated by this BH3-only protein. EMBO Rep. 2013;14:992–8.